Fundamental diagrams in traffic flow: the case of heterogeneous kinetic models

Gabriella Puppo*[1], Matteo Semplice†[2], Andrea Tosin‡[3] and Giuseppe Visconti§[1]

[1]Università dell'Insubria, Como, Italy
[2]Università degli Studi di Torino, Torino, Italy
[3]Istituto per le Applicazioni del Calcolo "M. Picone", CNR, Roma, Italy

August 1, 2014

Abstract

Experimental studies of vehicular traffic provide data on quantities like density, flux, and average speed of the vehicles. However, the diagrams that relate these variables can have different interpretations. In this paper, resting on the kinetic theory for vehicular traffic models, we introduce a new framework which takes into account the heterogeneous nature of the flow of vehicles. In more detail, we extend the model presented in [8] to the case of two populations of vehicles (such as e.g., cars and trucks), each with its own distribution function. Thus we consider traffic as a mixture of vehicles with different features, in particular different length and maximum speed. With this approach we can explain some interesting features of experimental diagrams. In fact, mathematical models for vehicular traffic typically yield fundamental diagrams that are single-valued functions of the density; in contrast, actual measurements show scattered data in the phase of congested traffic, which are naturally reproduced by our 2-population model as a result of the heterogeneous composition of the mixture of vehicles.

Keywords
Traffic flow, kinetic models, multispecies kinetic equations, fundamental diagrams

AMS subject classification 76P05, 65Z05, 90B20

1 Introduction

Prediction and control of traffic have become an important aspect in the modern world. In fact, the necessity to forecast the outflow time of a queue or to optimize traffic flows, thereby reducing the number of accidents, has arisen following the increase of circulating vehicles.

In the current mathematical literature, three different approaches are mainly used to model traffic flow phenomena. *Microscopic* models look at vehicles as single entities of traffic and they predict, using a system of ordinary differential equations, the evolution of their position and

*gabriella.puppo@uninsubria.it
†matteo.semplice@unito.it
‡a.tosin@iac.cnr.it
§giuseppe.visconti@uninsubria.it

speed (namely, the microscopic states characterizing their dynamics) regarded as time dependent variables. In these models, the acceleration is prescribed for each vehicle as a function of time, position, and speed of the various entities of the system, taking also into account mutual interactions among vehicles. For example, in the well known *follow-the-leader* model [12] each vehicle is assumed to adapt its speed to the one of the leading vehicle based on their instantaneous relative speed and mutual distance. On the opposite end, *macroscopic* models provide a large-scale aggregate point of view in which the focus is not on each single particle of the system. In this case, the motion of the vehicles along a road is described by means of partial differential equations inspired by conservation and balance laws from fluid dynamics, following the seminal works by Lighthill and Witham [22] and Richards [29]. Improvements and further evolutions of such a basic macroscopic description of traffic have been proposed over the years by several authors, from the classical mechanically consistent restatement of second order models by Aw and Rascle [3] to applications to road networks thoroughly developed in the book by Garavello and Piccoli [11]. In the middle, *mesoscopic* (or *kinetic*) models are based on a statistical mechanics approach, which still provides an aggregate representation of the traffic flow while linking macroscopic dynamics to pairwise interactions among vehicles at a smaller microscopic scale. These models will be the main reference background of the present paper. However, before entering the details of their discussion, some remarks about the other two types of models are in order.

Microscopic models give rise to very large systems of ordinary differential equations, when the number of vehicles is high, which makes the microscopic scale computationally not competitive. Moreover, the description of the behavior of single vehicles requires a quite detailed knowledge of several, mostly unknown or unaccessible, microscopic parameters while being often not really needed, since one usually is more interested in average quantities such as the flow rate or the mean speed. On the other hand, macroscopic models do not allow to account for interactions among vehicles, which instead play a prominent role in triggering traffic phenomena. A further drawback is that they typically require the prescription of closure laws linking the density and the flow (or the mean speed) of vehicles in order to give rise to self-consistent solvable equations (but see also [2]). This kind of information is usually recovered from interpolation or extrapolation of experimental data, which are then plugged into the mathematical models. Nevertheless one would like these data to be reproduced by models as a consequence of more fundamental modeling procedures rather than being postulated externally.

Kinetic (mesoscopic) models, first used by Prigogine [26, 27] and Paveri-Fontana [24], are based on the Boltzmann equation that describes the statistical behavior of a system of particles. From the kinetic point of view, the system is again seen as the resultant of the evolution of microscopic particles, with given microscopic position and speed, but its representation is provided in aggregate terms by a probability distribution, whose evolution is described by integro-differential equations. Compared to microscopic models, the kinetic approach requires a smaller number of equations and parameters. On the other hand, unlike macroscopic models, at the mesoscopic scale the evolution equations do not require an a priori closure law: the flow is provided by the statistical moments of the kinetic distribution function over the microscopic states. Kinetic models have also been extended to include multilane traffic flow [18, 19] and control problems [16], to name but just a few applications.

For an overview of vehicular traffic models at all scales, the interested reader is referred to the review papers by Bellomo and Dogbé [4], Klar and Wegener [20], and Piccoli and Tosin [25] and references therein.

In this paper we propose a multipopulation kinetic model for traffic flow, which draws inspiration from the ideas presented by Benzoni-Gavage and Colombo [5] recast in the frame of the discrete-velocity kinetic models by Delitala and Tosin [7] and Fermo and Tosin [8]. The main goal is to study fundamental diagrams, computed from moments of equilibrium solutions of the

kinetic equations, and in particular to show that taking into account the heterogeneous composition of the "mixture" of vehicles allows one to explain the experimentally observed scattering of such diagrams in the phase of congested traffic without invoking further elements of microscopic randomness of the system, cf. Fermo and Tosin [9]. In more detail, the structure of the paper is as follows: in Section 2 we briefly review the role of fundamental diagrams in vehicular traffic practice. Next, in Section 3 we describe the discrete-velocity kinetic model developed in [7, 8] by focusing on its spatially homogeneous version, which represents the mathematical counterpart of the experimental setting in which traffic equilibria and fundamental diagrams are measured. In Section 4 we first review the multi-population macroscopic model by Benzoni-Gavage and Colombo [5] and then introduce our new two-population kinetic model, proving in particular its consistency with the original single-population model and describing how to compute equilibrium solutions. Then in Section 5 we present and analyze the resulting fundamental diagrams, and we end in Section 6 with comments and perspectives.

2 Fundamental diagrams

In this section we present a brief description of a basic tool in the analysis of traffic problems, namely the diagrams which relate the macroscopic variables as density, flow and speed. The most used one is the so-called *fundamental diagram* which gives the flow of traffic as a function of its density. In traffic flow phenomena we can distinguish different regimes or *phases* of traffic, whose properties define the structure of the experimental diagrams. Here we describe the physical dynamics of traffic and the qualitative characteristics of the diagrams.

- Flow-density diagram: they report the flow rate of vehicles as a function of the number of vehicles per unit length (density). At low traffic densities, the flow of vehicles grows linearly with the density and this regime is called *free phase flow*, in which the interactions between vehicles are rare. There is a value of the density, called *critical density*, at which the flow reaches its maximum value. Beyond the critical density we have the *congested phase* of traffic which is defined by Kerner in [17] as complementary to the phase of free flow. In this regime the flow decreases as the density increases. In fact, faster vehicles are impeded by slower ones and the formation of local slowdowns (*phantom traffic jam*) is first observed. Additional increments of the density cause a steady reduction in the flow until the so-called *traffic jam* is reached, in which the density reaches its maximum value, called *jam density*, and the flow is zero.

- Speed-density diagram: they give the typical velocity of a vehicle as a function of the local density of traffic. In free flow conditions, the vehicles travel at the maximum speed allowed, that depends on the infrastructure, on the mechanical characteristics of the vehicle and on speed limits. This speed can be reached when there is a large distance between vehicles on the road and the maximum speed is called *free flow speed*. Instead, in congested flow conditions the vehicles travel closer, at a reduced speed, until the density reaches the jam density, at which vehicles stop and have zero speed.

The diagrams previously described play an important role in the prediction of the capacity of a road and in the control of the flow of vehicles.

Examples of fundamental diagrams provided by experimental measurements are shown in Figure 1. They clearly exhibit the phase transition between free and congested flow: below the critical density the flow values can be approximately represented by a line with a positive slope and thus the flow appears as a single-valued increasing function of the density, with a

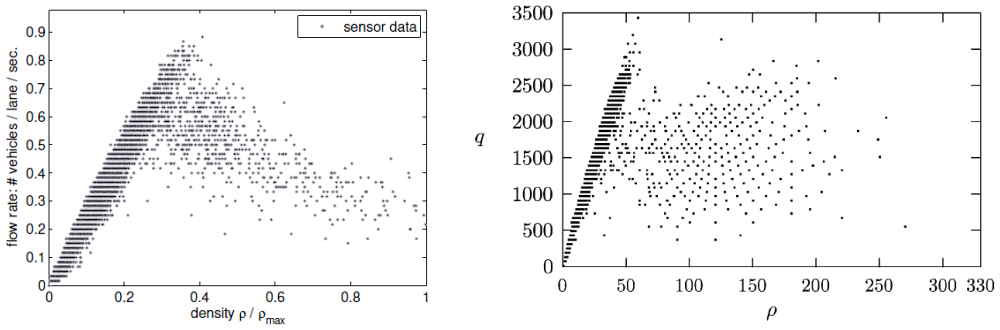

Figure 1: Fundamental diagrams obtained from experimental data. On the left, measurements provided by the Minnesota Department of Transportation in 2003, reproduced by kind permission from Seibold et al. in [30]; on the right, experimental data collected in one week in viale del Muro Torto, Roma, Italy, and shown by Piccoli and Tosin in the review [25].

low, but non zero, dispersion; above the critical density, the flow decreases and exhibits a large scattering of the data resembling a stochastic process. In this stage, therefore, the flow cannot be represented as a single-valued function of the density.

We will consider kinetic models of traffic flow because they naturally provide a sharp transition from the free to the congested phase of traffic. However, even standard kinetic models do not account for the scattered data typical of the congested regime. Usually, this behavior of the flow is explained considering the individuality of the drivers, who may decide to drive at a different speed than the one resulting from the local density.

In this work, we introduce a kinetic model as a mixture of different populations of vehicles, for instance cars and trucks, each described by its own distribution function. With this extension, we believe that the scattered data can be naturally accounted for using the heterogeneous composition of the flow.

3 A discrete kinetic model

In this section we briefly revisit a kinetic traffic model recently introduced in [8]. In the kinetic approach we focus on a statistical description of the microscopic states of the particles, therefore the evolution of the position x and velocity v of the vehicles is described by means of a distribution function $f = f(t, x, v)$ such that $f(t, x, v)dxdv$ is the number of vehicles between x and $x + dx$ with velocity between v and $v + dv$.

The model proposed in [8] is a kinetic model which is discrete both in space and in velocity, thus let X_i be the i-th space cell which identifies a portion of the road and v_j the j-th velocity class. The authors introduce $f = f_{ij}(t)$, the distribution function of vehicles that are located, at time t, in cell X_i with speed v_j. Moreover, let $X \subseteq \mathbf{R}$ be the spatial domain and $V \subseteq \mathbf{R}^+$ the microscopic speed domain, we have $X = \cup_{i=1}^m X_i$ and $V = \{v_j\}_{j=1}^n$ with $0 \leq v_j < v_{j+1}, \forall j = 1, \ldots, n$ and $v_1 = 0, v_n = V_{\max}$, where $V_{\max}$ is the maximum speed of a vehicle. Thus $V_{\max}$ can be chosen as a speed limit imposed by safety regulations, or by the state of the road, or by the mechanical characteristics of the vehicle. Therefore, each microscopic state (x_i, v_j) belongs to the space of discrete states $X \times V$. The kinetic distribution f can be recovered from $f_{ij} : [0, T_{\max}] \to \mathbb{R}^+$, $i = 1, \ldots, m$, $j = 1, \ldots, n$ as:

$$f(t,x,v) = \sum_{i=1}^{m}\sum_{j=1}^{n} f_{ij}(t)\chi_{X_i}(x)\delta_{v_j}(v) \tag{1}$$

thus f is an atomic distribution with respect to the variable v and it is piecewise constant with respect to the variable x. The macroscopic variables, vehicle density ρ, flux q and average speed u, useful in the study of traffic, are obtained from the kinetic model as distributional moments of (1) with respect to v:

$$\rho(x,t) = \sum_{j=1}^{n} f_{ij}(t), \qquad q(x,t) = \sum_{j=1}^{n} v_j f_{ij}(t), \qquad u(x,t) = \frac{q(x,t)}{\rho(x,t)}. \tag{2}$$

The experimental diagrams are constructed assuming that traffic flow is stationary and homogeneous in space, thus density and flow are computed from the equilibrium distributions $\left\{f_j^e\right\}_{j=1}^n$. To this end, we investigate the evolution of the distribution functions, due only to vehicle interactions, and then we look at the equilibria of the model. Thus, we can take into account the spatially homogeneous case, in which the density and the flux are assumed to be uniform in space, and we define analytically the fundamental and the speed diagrams with the following maps:

$$\rho \to q(\rho) = \sum_{j=1}^{n} v_j f_j^e, \quad \rho \to u(\rho) = \frac{q(\rho)}{\rho}. \tag{3}$$

In particular, if for any given ρ the system (4) admits a unique stable equilibrium then these maps are actual functions of ρ; otherwise, they define multivalued diagrams. We remark that the map $q(\rho)$ is not based on a priori closure relations, as opposed to macroscopic models, but it is obtained by the large time evolution of the kinetic distribution function.

For the homogeneous case we can drop the dependence on i, writing $f_{ij} \equiv f_j$, $\forall i = 1,\dots,m$ and the model proposed in [8] reduces to

$$\frac{df_j}{dt} = J_j(f,f), \qquad j = 1,\dots,n, \tag{4}$$

where $J_j(f,f)$ is called collisional operator and it simulates the microscopic interactions between vehicles that determine the change of f_j with respect to time. Conservation of mass requires that:

$$\sum_{j=1}^{n} J_j(f,f) = 0 \tag{5}$$

in fact, we have:

$$\sum_{j=1}^{n} \frac{df_j}{dt} = \frac{d}{dt}\sum_{j=1}^{n} f_j = \frac{d\rho}{dt} = 0.$$

This means that in the space homogeneous case ρ can be considered as a parameter of the system (4), because it is fixed by the initial conditions and it remains constant during the evolution of the distribution function f_j, so:

$$\rho = \sum_{j=1}^{n} f_j(0) = \sum_{j=1}^{n} f_j^e$$

where $\{f_j(0)\}_{j=1}^n$ are the initial conditions of the system (4) and $\left\{f_j^e\right\}_{j=1}^n$ is the equilibrium state of the system such that $J_j(f^e, f^e) = 0$, $\forall j = 1, \ldots, n$.

The collisional operator $J_j(f, f)$ models the microscopic interactions between vehicles. As in [8], the description of $J_j(f, f)$ is based on stochastic game theory: vehicles are the players, their velocities are the game strategies and the post-interaction velocities are the payoff of the game. This technique allows us to assign a post-interaction velocity in a non-deterministic way. We report here the construction of the collisional operator which will be extended later to the 2-population case. We consider only binary interactions, thus the collisional operator can be written as:

$$J_j(f, f) = \eta \sum_{h,k=1}^{n} A_{h,k}^j f_h f_k - \eta f_j \sum_{k=1}^{n} f_k$$

where $G_j = \eta \sum_{h,k=1}^n A_{h,k}^j f_h f_k$ and $L_j = \eta f_j \sum_{k=1}^n f_k$ are the gain and loss terms respectively. In the gain term, we call candidate the vehicle which modifies its velocity v_h in the test speed v_j after an interaction with the field vehicle that travels at the velocity v_k. Instead, the term L_j describes the loss of speed v_j after an interaction with any field vehicle.

In this work, we will assume that η, the rate of interactions, is constant, but it could also depend on the relative velocity of the interacting vehicles, so $\eta = \eta(|v_h - v_k|)$. The matrix $A^j = \left\{A_{h,k}^j\right\}_{h,k=1}^n$, $j = 1, \ldots, n$ is called table of games and it gives the discrete probabilities to gain the test speed v_j, thus:

$$A_{h,k}^j = \mathbb{P}(v_h \to v_j | v_k), \quad \forall h, k, j = 1, \ldots, n$$

and they fulfill the following conditions:

$$0 \leq A_{h,k}^j \leq 1, \quad \forall j \text{ and } h, k = 1, \ldots, n$$
$$\sum_{j=1}^{n} A_{h,k}^j = 1, \quad h, k = 1, \ldots, n,$$

which express the fact that, for each fixed h, k, $A_{h,k}^j, j = 1, \ldots, n$ defines a discrete probability distribution. This means that some velocity v_j will result from the interaction between v_h and v_k, and furthermore it ensures that (5) holds.

Let $V_{\max} = v_n$ be the maximum velocity, and $\rho_{\max}$ be the road capacity, i.e. the number of vehicles on the road in bumper-to-bumper condition. Since any speed variation depends on the local road congestion and on the quality of the road, the table of games of the model (4) is built using the following assumptions:

- a candidate vehicle with velocity v_h can accelerate only to v_{h+1}, but it can decelerate down to $v_j = v_k$ when it interacts with a field vehicle with lower velocity v_k;
- let P be the probability that a vehicle obtains the maximum test velocity resulting from an interaction, then P is proportional to the fraction of free road ahead through a coefficient $\alpha \in [0, 1]$, thus $P = \alpha\left(1 - \frac{\rho}{\rho_{\max}}\right)$. We can think of α as a parameter describing the state of the road, with $\alpha = 1$ for optimal road conditions.

We distinguish three cases:

1. interaction with a faster field vehicle: in this case we have $h < k$. Following the interaction the candidate vehicle can maintain its velocity or it can accelerate. So the microscopic test speed is $v_j = v_{h+1}$ with probability P, while $v_j = v_h$ with probability $1 - P$. In other words,

$$A^j_{h,k} = \begin{cases} 1-P & \text{if } j = h \\ P & \text{if } j = h+1 \\ 0 & \text{else} \end{cases} \qquad k = 2, \ldots, n,\ h < k \tag{6}$$

2. interaction with a slower field vehicle: in this case we have $h > k$. Following the interaction the candidate vehicle v_h can maintain its velocity with probability P, thus overtaking the leading field vehicle, or it decelerates to the velocity v_k with probability $1 - P$. So the transition probability allows to assume the microscopic test speeds $v_j = v_k$ or $v_j = v_h$, thus

$$A^j_{h,k} = \begin{cases} 1-P & \text{if } j = k \\ P & \text{if } j = h \\ 0 & \text{else} \end{cases} \qquad k = 1, \ldots, n-1,\ h > k \tag{7}$$

3. interaction with a field vehicle which has the same velocity: $v_h = v_k$. The candidate vehicle can assume the microscopic test speed $v_j = v_h$, thus maintaining the pre-interaction velocity if it is not disturbed by the leading vehicle; it can accelerate to $v_j = v_{h+1}$ overtaking the field vehicle with probability P or it can decelerate to $v_j = v_{h-1}$ with probability Q. It is reasonable to assume that a vehicle interacting with another vehicle with the same velocity will decrease its microscopic speed with probability proportional to the state of the occupation of the road $\frac{\rho}{\rho_{\max}}$, with a constant of proportionality depending on the bad state of the road, i.e. $1 - \alpha$. So we take $Q = (1-\alpha)\frac{\rho}{\rho_{\max}}$. We further distinguish three cases, in fact if the vehicles have the velocity $v_1 = 0$ or the maximum velocity v_n then the candidate vehicle cannot decelerate or accelerate, respectively. Thus:

$$A^j_{1,1} = \begin{cases} 1-P & \text{if } j = 1 \\ P & \text{if } j = 2 \\ 0 & \text{else} \end{cases} \tag{8}$$

$$A^j_{h,h} = \begin{cases} Q & \text{if } j = h-1 \\ 1-(P+Q) & \text{if } j = h \\ P & \text{if } j = h+1 \\ 0 & \text{else} \end{cases} \qquad h = 2, \ldots, n-1 \tag{9}$$

$$A^j_{n,n} = \begin{cases} Q & \text{if } j = n-1 \\ 1-Q & \text{if } j = n \\ 0 & \text{else} \end{cases} \tag{10}$$

In this way the collision term is completely defined.

We study the evolution to equilibria of a given initial condition corresponding to a fixed value of ρ until the equilibrium state is reached. In this fashion we obtain the fundamental and the

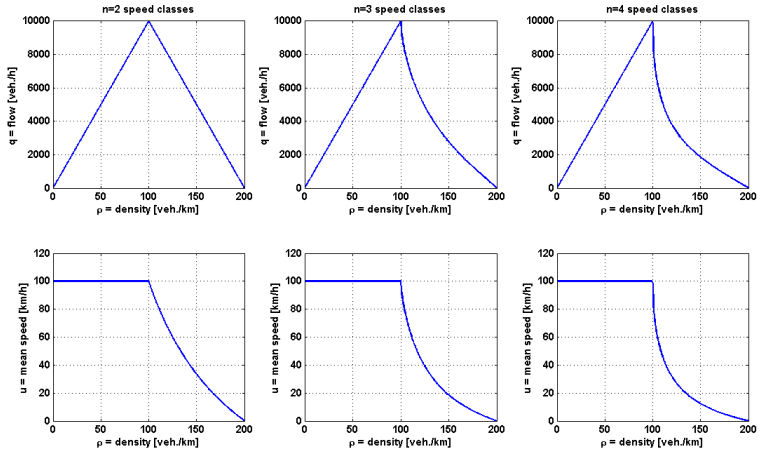

Figure 2: Fundamental diagrams (top row) and speed diagrams (bottom row) obtained from the model (4) with $n = 2$ (left), $n = 3$ (center) and $n = 4$ (right) velocity classes. We choose $\rho_{\max} = 200$veh./km and the microscopic velocity are uniformly distributed $\left\{v_j = \frac{j-1}{n-1} V_{\max}\right\}_{j=1}^{n}$ with $V_{\max} = 100$km/h.

speed diagrams of Figure 2: if $\rho < \frac{1}{2}\rho_{\max}$ we have a free phase of traffic in which the flow, defined as number of vehicles per time, is an increasing linear function of the density, in fact the asymptotic distribution can be obtained analitically, and is given by ([9])

$$f_{ij} = \begin{cases} 0 & j < n \\ \rho & j = n \end{cases}$$

i.e. all cars achieve the maximum velocity; instead, if $\rho > \frac{1}{2}\rho_{\max}$ we have a congested phase of traffic which depends on the number n of velocity classes; for instance, if we consider $n = 2$, the flow is a decreasing linear function but if we consider $n \geq 2$, the flow decreases non-linearly. Here $\rho_c = \frac{1}{2}\rho_{\max}$ is the critical density.

The model (4) confirms that the kinetic approach is able to catch successfully the phase transition from free to congested traffic flow, when the critical density ρ_c is reached, without the need of providing an heuristic closure to give the flux as a function of the density.

However, the model (4) provides again a single-valued density-flux relation. In fact, as shown in [9], $\forall \rho \in [0, \rho_{\max}]$ there exists a unique equilibrium point of the system (4) which is stable and attractive: given the initial conditions $\{f_j(0)\}_{j=1}^{n}$ such that $\sum_{j=1}^{n} f_j(0) = \rho$, it is possible to prove that the n equilibrium values $\left\{f_j^e\right\}_{j=1}^{n}$ do not depend on the initial distribution and consequently the flux $q(\rho)$ is uniquely determined by the initial density ρ, which does not explain the scattered data of experimental diagrams.

4 Two-population models

Starting from the kinetic approach introduced in the previous section, here we introduce a model which treats traffic as a mixture of two (or more) populations with different features. As

far as we know, this is the first attempt to account for the heterogeneity of traffic in a kinetic model. We will see that this structure allows to understand the nature of scattered data in experimental diagrams. For the sake of simplicity we will consider a 2-population model, but the model can be easily extended to more complex mixtures.

In recent literature, multi-population models of vehicular traffic have already been successfully proposed. In [5] the authors proposed an n-population generalization of the Lighthill-Whitham [22] and Richards [29] traffic models. Here, we illustrate the case for $n = 2$ species:

$$\begin{cases} \partial_t \rho_1 + \partial_x \left(F_1(\rho_1, \rho_2) \right) = 0 \\ \partial_t \rho_2 + \partial_x \left(F_2(\rho_1, \rho_2) \right) = 0 \end{cases} \tag{11}$$

where $F_i(\rho_1, \rho_2) = \rho_i v_i(\rho_1, \rho_2)$ is the flux function of the i-th population, $v_i(\rho_1, \rho_2)$ is the speed-density relation which describes the attitude of drivers to change their speed with respect to the local values of ρ_1 and ρ_2. We note that this model can be written in terms of a parameter s, which we call the fraction of road occupancy, defined as $s = \rho_1 l_1 + \rho_2 l_2$, where ρ_1, ρ_2 are the local traffic densities, and $l1$, $l2$ are the characteristic lengths of the vehicles in the two populations. In [5] v_i is taken from the usual Greenshield's law [10, 31], therefore:

$$v_i(\rho_1, \rho_2) = (1 - s)\, V_i, \quad i = 1, 2$$

where V_i is the maximum speed of the i-th population. The system of conservation laws (11) becames:

$$\begin{cases} \partial_t \rho_1 + \partial_x \left((1 - s) V_1 \rho_1 \right) = 0 \\ \partial_t \rho_2 + \partial_x \left((1 - s) V_2 \rho_2 \right) = 0. \end{cases} \tag{12}$$

The flux is given by

$$\mathbf{F} = [(1 - s)V_1\rho_1, (1 - s)V_2\rho_2]$$

and we notice that, given ρ, the total flux of vehicles is $F_1 + F_2$, and this expression takes different values depending on the initial data ρ_1, ρ_2, such that $\rho_1 l_1 + \rho_2 l_2 = s$.

4.1 A two-population kinetic model

Now, we extend the construction of [8] introducing a model with two populations to take into account the natural heterogeneous composition of traffic. For simplicity, we consider only two populations, but the model can be easily extended to mixtures with more components. Again, we limit the study to the spatially homogeneous case in order to construct fundamental diagrams. To distinguish the two classes of vehicles, we will refer to them as *cars* and *trucks*.

The first difference that we introduce between vehicles is given by the different maximum velocity; therefore if $V_C = \left\{ v_j = \frac{j-1}{n-1} v_n \right\}_{j=1}^{n}$ is the space of discrete microscopic speeds related to cars, with $v_1 = 0$, $v_i < v_{i+1}$, $\forall\, i$ (v_n is the maximum speed), we suppose that the space of discrete microscopic speeds related to trucks is such that $V_T \subset V_C$, so $V_T = \left\{ v_j = \frac{j-1}{n-1} v_n \right\}_{j=1}^{m}$, where m is an integer such that $m \in \{1, \ldots, n\}$.

Let $f = f_j(t)$, $g = g_j(t)$ be the distribution functions of cars and trucks respectively with a velocity in the j-th class, then

$$\begin{aligned} N_{C,j} &= L f_j, \quad j = 1, \ldots, n \\ N_{T,j} &= L g_j, \quad j = 1, \ldots, m \end{aligned} \tag{13}$$

are the total number of cars and trucks (or particle number) with velocity v_j, where L is the length of the section of road we are considering. The total number of vehicles is given by

$$N = N_C + N_T = L\sum_{j=1}^{n} f_j + L\sum_{j=1}^{m} g_j.$$

The maximum number of cars and trucks which can be accomodeted in the road is

$$N_C^{\max} = \frac{L}{l_C}, \quad N_T^{\max} = \frac{L}{l_T}$$

where l_C, l_T are the average lengths of vehicles that are in the class of cars and in the class of trucks respectively. This however corresponds to the case in which the road is occupied only by one of the two classes of vehicles. Let $N_C l_C$ and $N_T l_T$ be the spaces occupied by cars and trucks, while $S = N_C l_C + N_T l_T$ is the total space occupied in the road section. If we rescale with respect to L, we obtain the fraction of occupied space:

$$0 \leq s = \frac{N_C l_C + N_T l_T}{L} \leq 1. \tag{14}$$

We define the kinetic distribution functions of the two populations as:

$$f(t,v) = \sum_{j=1}^{n} f_j(t)\delta_{v_j}(v), \quad g(t,v) = \sum_{j=1}^{m} g_j(t)\delta_{v_j}(v).$$

where again we are considering an atomic distribution with respect to the discrete velocities. If we consider their moments with respect to v, we obtain the macroscopic quantities:

- for the class of cars:

$$\rho_C(t) = \sum_{j=1}^{n} f_j(t), \qquad q_C(t) = \sum_{j=1}^{n} v_j f_j(t), \qquad u_C(t) = \frac{q_C(t)}{\rho_C(t)} \tag{15}$$

- for the class of trucks:

$$\rho_T(t) = \sum_{j=1}^{m} g_j(t), \qquad q_T(t) = \sum_{j=1}^{m} v_j g_j(t), \qquad u_T(t) = \frac{q_T(t)}{\rho_T(t)}. \tag{16}$$

where ρ_C, ρ_T are the number densities, q_C, q_T are the marcoscopic fluxes and u_C, u_T the average speeds of the two species. Thus $N_C = L\rho_C$ and $N_T = L\rho_T$.

We can rewrite (14), using the macroscopic variables, as:

$$0 \leq s = \rho_C l_C + \rho_T l_T \leq 1. \tag{17}$$

In the single-population kinetic model (4), the probability transitions depend on the rate of the local density ρ and on α, i.e. on the state of the road. In our 2-population model, instead, the probability transitions will depend on the fraction of occupied space s, defined in (17), which is the natural generalization of $\frac{\rho}{\rho_{\max}}$, and on α.

The evolution of f_j and g_j in the space homogeneous case is given by:

$$\frac{df_j}{dt} = J_j^C(f,g), \quad j = 1,\dots,n$$
$$\frac{dg_j}{dt} = J_j^T(g,f), \quad j = 1,\dots,m$$

where $J_j^C(f,g)$ and $J_j^T(g,f)$ are the collisional operators that account for the interactions in which cars respectively trucks are the candidate vehicles. Since we consider only binary interactions, we can follow an approach frequently used to describe the mixture of two gases in kinetic theory, see for instance [15, 6, 13], writing each collisional operator as the sum of two terms:

$$J_j^C(f,g) = J_j^{C,C}(f,f) + J_j^{C,T}(f,g), \quad j = 1,\dots,n.$$

The two terms describe the binary interactions of a car as candidate vehicle with a field vehicle which is either a car or a truck respectively. Each of the two single collisional operators will be written with the same logic of the single population model, but keeping in mind that the dimension of the matrices representing the tables of games will be different:

$$J_j^{C,C}(f,f) = \eta \sum_{h,k=1}^{n} A_{h,k}^j f_h f_k - \eta f_j \sum_{k=1}^{n} f_k, \quad j = 1,\dots,n$$
$$J_j^{C,T}(f,g) = \eta \sum_{h=1}^{n}\sum_{k=1}^{m} B_{h,k}^j f_h g_k - \eta f_j \sum_{k=1}^{m} g_k, \quad j = 1,\dots,n.$$

Similarly:

$$J_j^T(g,f) = J_j^{T,T}(g,g) + J_j^{T,C}(g,f), \quad j = 1,\dots,m.$$

Here the first term describes the binary interactions of a truck with a truck, while the second one describes the interaction in which trucks react with cars. Then the single collisional operator can be written as:

$$J_j^{T,T}(g,g) = \eta \sum_{h,k=1}^{m} C_{h,k}^j g_h g_k - \eta g_j \sum_{k=1}^{m} g_k, \quad j = 1,\dots,m$$
$$J_j^{T,C}(g,f) = \eta \sum_{h=1}^{m}\sum_{k=1}^{n} D_{h,k}^j g_h f_k - \eta g_j \sum_{k=1}^{n} f_k, \quad j = 1,\dots,m.$$

Finally, our 2-populations kinetic model will be defined by the equations:

$$\begin{aligned}
\frac{df_j}{dt} &= \eta \left(\sum_{h,k=1}^{n} A_{h,k}^j f_h f_k + \sum_{h=1}^{n}\sum_{k=1}^{m} B_{h,k}^j f_h g_k - f_j \left(\sum_{k=1}^{n} f_k + \sum_{k=1}^{m} g_k \right) \right), \quad j = 1,\dots,n \\
\frac{dg_j}{dt} &= \eta \left(\sum_{h,k=1}^{m} C_{h,k}^j g_h g_k + \sum_{h=1}^{m}\sum_{k=1}^{n} D_{h,k}^j g_h f_k - g_j \left(\sum_{k=1}^{n} f_k + \sum_{k=1}^{m} g_k \right) \right), \quad j = 1,\dots,m
\end{aligned} \tag{18}$$

where A^j, B^j, C^j, D^j are the tables of games that give the probabilities of the transitions between different states of system (18), i.e. the probabilities that candidate vehicles get the microscopic test speeds v_j after interacting with field vehicles. They fulfill the following assumptions:

$$0 \le A_{h,k}^j, B_{h,k}^j, C_{h,k}^j, D_{h,k}^j \le 1, \quad \forall\, h,k,j$$
$$\sum_{j=1}^{n} A_{h,k}^j = \sum_{j=1}^{n} B_{h,k}^j = \sum_{j=1}^{m} C_{h,k}^j = \sum_{j=1}^{m} D_{h,k}^j = 1, \quad \forall\, h,\, k,$$

and the two sets of equations describe the fact that the interaction of a vehicle with velocity v_h with a vehicle of velocity v_k results in one of the possible velocities v_j with probability 1. As a consequence of these assumptions, summing over j each of the two equations (18) results in mass conservation for each of the species, namely

$$\frac{d}{dt}\sum_{j=1}^{n} f_j = 0, \quad \frac{d}{dt}\sum_{j=1}^{m} g_j = 0$$

which is equivalent to

$$\frac{d\rho_C}{dt} = \frac{d\rho_T}{dt} = 0.$$

The tables of games are constructed with the same ansatz of the original model, but now the probabilities P and Q that an interaction occurs will depend on the fraction of space s in the road which is occupied by the mixture, i.e. $P = \alpha(1-s)$ and $Q = (1-\alpha)s$. It is through the parameter s that the two populations exchange information. The tables A^j, C^j have the same construction as in (6), (7), (8), (9), (10), because they are the discrete probability distributions in which the two involved players belong to the same class of vehicles except that A^j is an $n \times n$ matrix $\forall\, j = 1, \ldots, n$ and C^j is an $m \times m$ matrix $\forall\, j = 1, \ldots, m$.

The tables B^j and D^j represent the interactions between the two populations. In particular, the table B^j is the discrete probability distribution in which the candidate cars change their velocity v_h in the microscopic test speed v_j after an interaction with the field trucks with velocity v_k. If $h < k,\ h > k$ and $h = k = 1$ we get the same rules introduced in (6), (7) and (8); while we rewrite the other cases in order to obtain a consistent 2-population model if $l_C = l_T$ and $n = m$, i.e. the two classes of vehicles have the same maximum speed:

$$B^j_{h,h} = \begin{cases} Q & \text{if } j = h-1 \\ 1-(P+Q) & \text{if } j = h \\ P & \text{if } j = h+1 \\ 0 & \text{else} \end{cases} \qquad h = 2, \ldots, m < n$$

and we remark that if $h = k = m < n$ cars can accelerate to a test velocity higher than v_m. On the other hand, if $m = n$, we have the following probabilities

$$B^j_{n,n} = \begin{cases} Q & \text{if } j = n-1 \\ 1-Q & \text{if } j = n \\ 0 & \text{else} \end{cases} \qquad h = n = m.$$

Note that B^j, $\forall\, j = 1, \ldots, n$ is an $n \times m$ matrix.

The table D^j, instead, is the discrete probability distribution in which the candidate truck changes its velocity v_h in the microscopic test speed v_j after an interaction with a field car with velocity v_k. If $h > k$ and $h = k$ we have the same rules introduced in (7), (8), (9), (10), while if $m = h < k$ trucks can't accelerate because they already have the maximum speed v_m, therefore:

$$D^j_{h,k} = \begin{cases} 1 & \text{if } j = h \\ 0 & \text{else} \end{cases} \qquad h = m < k \in \{m+1, \ldots, n\}$$

$$D^j_{h,k} = \begin{cases} 1-P & \text{if } j = h \\ P & \text{if } j = h+1 \\ 0 & \text{else} \end{cases} \qquad h < k < m$$

then D^j, $\forall\, j = 1, \ldots, m$ are $m \times n$ matrices.

Finally, we prove that the 2-population kinetic model (18) satisfies a fundamental property which has already been studied in kinetic models for mixture of gases. In [1] a consistent BGK-type model for gas mixtures is proposed, which fulfills an *indifferentiability principle*: when all the species of gas are identical one can recover the equation for a single component gas. In traffic flow models the indifferentiability principle can be stated in the following Theorem which ensures that the 2-population model (18) and the 1-population model (4) are consistent.

Theorem 4.1 (Indifferentiability principle)**.** *Suppose the vehicles in the two populations have the same length and the same space of discrete velocities, then the total distribution function $F_j = f_j + g_j$, $\forall j = 1, \ldots, n$, obeys the evolution equations of the single-population model (4).*

Proof. Since the discrete velocity spaces are identical, in particular $m = n$. Let $l = l_C = l_T$ and $\rho_{\max} = \frac{1}{l}$. Then, $s = (\rho_C + \rho_T)\, l = \frac{(\rho_C + \rho_T)}{\rho_{\max}}$. Therefore, the matrices are all equal, $A^j \equiv B^j \equiv C^j \equiv D^j$, $\forall j$. Let f_j and g_j be the distribution functions of the two classes of vehicles with speed in the j-th velocity class. Summing their evolution equations, we easily get:

$$\frac{d(f_j + g_j)}{dt} = \sum_{h,k=1}^{n} A^j_{hk}\,(f_h + g_h)\,(f_k + g_k) - (f_j + g_j) \sum_{k=1}^{n} (f_k + g_k)\,, \quad j = 1, \ldots, n$$

which is the evolution equation of the 1-population kinetic model (4), with distribution function given by $F_j = f_j + g_j$. □

Remark 4.2. In [1] the indifferentiability principle is proven for a model constructed with a single collision operator, which hinders the description of the separate interactions with particles of different species in the mixture. In more standard models for gas mixtures, the collision terms are separate, as in our case, but the indifferentiability principle holds only at equilibrium. Here, instead, Theorem 4.1 holds for all time, without the need of merging the two collision terms into one.

4.2 A well-balanced formulation for computing equilibria

Our numerical evidence suggests that, for any couple of initial densities ρ_C and ρ_T, any initial distribution $f_j(0), g_j(0)$, such that $\sum f_j(0) = \rho_C$ and $\sum g_j(0) = \rho_T$, converges to the same couple of equilibrium distributions f^e_j, g^e_j, which is therefore uniquely determined by ρ_C and ρ_T. To get the correct equilibrium, however, it is important to devise a well balanced scheme. As we will see, round off error can drive the solution to equilibrium states which are obviously spurious, if the model is not integrated properly.

In some simplified cases, it is possible to write analytic expressions for the equilibrium distributions, shedding light on the structure of fundamental diagrams. In [8] the well-posedness of the system (4) and the existence of equilibria was established. There, equilibrium states are computed analytically, in some simplified cases. Here, we will integrate numerically the system of ODE's.

In the remaining part of this paper, we will always assume that the parameter α which represents the state of the road is always set to one. From a modelling point of view, we will assume that the quality of the road does not interfere with the flow of traffic. In this case $P = 1 - s$ and $Q = 0$. This simplifies the structure of the interaction matrices, but nonetheless the wealth of information which can be derived from this model is quite surprising.

The evolution equations for the two distribution functions are integrated in time with an ODE solver, until steady state is reached. The system can be written out explicitly in matrix

form. For the sake of completeness, we write the interaction matrices in the case $\alpha = 1$. Further, let $t = 1 - s$. We write only the non zero elements of the matrices, drawing a circle around the elements on the j-th column and on the j-th row of each matrix. The first two matrices for the interaction between cars are

$$A^1 = \begin{bmatrix} \textcircled{s} & \textcircled{s} & \textcircled{s} & \dots & \textcircled{s} \\ \textcircled{s} & & & & \\ \textcircled{s} & & & & \\ \vdots & & & & \\ \textcircled{s} & & & & \end{bmatrix} \qquad A^2 = \begin{bmatrix} t & \textcircled{t} & t & \dots & t \\ \textcircled{t} & \textcircled{s} & \textcircled{s} & \dots & \textcircled{s} \\ & \textcircled{s} & & & \\ & \vdots & & & \\ & \textcircled{s} & & & \end{bmatrix} \tag{19}$$

We also write the generic matrix A^j and the last matrix A^n

$$A^j = \begin{bmatrix} & & & t & \textcircled{t} & \dots & t \\ \textcircled{t} & \dots & \textcircled{t} & \textcircled{s} & \dots & \textcircled{s} \\ & & & \textcircled{s} & & & \\ & & & \vdots & & & \\ & & & \textcircled{s} & & & \end{bmatrix} \qquad A^n = \begin{bmatrix} & & & & & \\ & & & & & \\ & & & & t & t \\ \textcircled{t} & \dots & \textcircled{t} & \textcircled{t} & \textcircled{1} \end{bmatrix} \tag{20}$$

The matrices A^j are all $n \times n$. The matrices C^j have exactly the same structure, except that they are $m \times m$. The interaction matrices B^j are $n \times m$. They have the same structure of the A^j's, except when $j = m, m+1$, or in general $j > m$:

$$B^m = \begin{bmatrix} & & t & \textcircled{t} \\ \textcircled{t} & \dots & \textcircled{t} & \textcircled{s} \\ & & & \textcircled{s} \\ & & & \vdots \\ & & & \textcircled{s} \end{bmatrix} \qquad B^{m+1} = \begin{bmatrix} & & & t \\ \textcircled{t} & \dots & \dots & \textcircled{t} \\ & & & \end{bmatrix} \qquad B^j = \begin{bmatrix} & & & \\ \textcircled{t} & \dots & \dots & \textcircled{t} \\ & & & \end{bmatrix}. \tag{21}$$

Finally, the D^j are $m \times n$. Again, they can be easily derived from the A^j. The only case which is different is D^m,

$$D^m = \begin{bmatrix} & & & & & \\ & & & & & \\ & & t & \textcircled{t} & \dots & t \\ \textcircled{t} & \dots & \textcircled{t} & \textcircled{1} & \textcircled{1} & \textcircled{1} \end{bmatrix} \tag{22}$$

Note the sparsity pattern of these matrices, which easily allows for a fast evaluation of he collision term.

In [9], the analytic equilibrium solutions are computed by substituting the sum of the distribution functions with the corresponding density in the loss term. In fact, in the spatially homogeneous case, the density is steady in time, thus it can be considered as a parameter of the ODE's system.

This simplification cannot be carried out when the system is integrated numerically, because of instabilities triggered by round-off. This phenomenon is indeed quite surprising, but interesting.

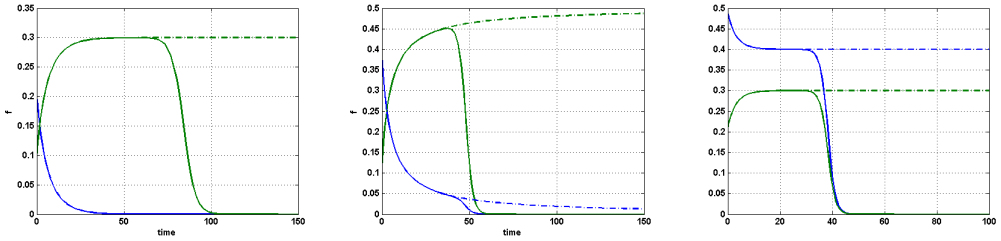

Figure 3: Solution obtained with (dashed line) and without (continuous line) the well balanced formulation to solve the space homogeneous case. Left $s = 0.3$, center $s = 0.5$, right $s = 0.7$

For the sake of simplicity, we illustrate this problem for the 1-population model (4), but our considerations apply also to the 2-population framework. We can write the 1 population model in the two equivalent formulations:

$$\frac{df_j}{dt} = \sum_{h,k=1}^{n} A_{hk}^j f_h f_k - f_j \sum_{k=1}^{n} f_k, \quad j = 1, \dots, n \tag{23}$$

$$\frac{df_j}{dt} = \sum_{h,k=1}^{n} A_{hk}^j f_h f_k - \rho f_j, \quad j = 1, \dots, n. \tag{24}$$

However, integrating the equations numerically the two formulations are not equivalent. It is easy to verify that (23) leads to the correct steady state solutions (we will call this formulation "well balanced"), while (24) does not preserve stationary solutions and eventually it even leads to a violation of mass conservation. This situation is similar to the construction of well-balanced schemes for balance laws, where particular care is needed to preserve stationary solutions at the discrete level, e.g. see the article of Leveque [21] and the more recent work of Noelle-Xing-Shu [23], and references therein, where the huge literature on this issue is accounted for.

Here we illustrate the case with $n = 2$ velocity classes, but the same behavior can be observed for $n > 2$. Let P and Q be the probability transitions introduced in the previous section, then the formulation (23) becomes:

$$\begin{cases} \dfrac{df_1}{dt} = f_1 \left[-P f_1 + (1 - 2P) f_2 \right] + Q f_2^2 \\ \dfrac{df_2}{dt} = f_2 \left[(2P - 1) f_1 - Q f_2 \right] + P f_1^2 \end{cases}$$

and summing the two equations it is easy to see that $d(f_1 + f_2)/dt \equiv 0$, so that $f_1 + f_2$ is constant in time, therefore for any given initial density ρ_0 and $\forall t$ we have that $\rho(t) = f_1(t) + f_2(t) = f_1(0) + f_2(0) = \rho_0$.

Conversely, the formulation (24) of the single population model can be written for the case $n = 2$ as:

$$\begin{cases} \dfrac{df_1}{dt} = f_1 \left[(1 - P) f_1 + 2(1 - P) f_2 - \rho_0 \right] + Q f_2^2 \\ \dfrac{df_2}{dt} = f_2 \left[2P f_1 + (1 - Q) f_2 - \rho_0 \right] + P f_1^2 \end{cases}$$

from which we obtain the evolution equation for the sum of the two distribution functions:

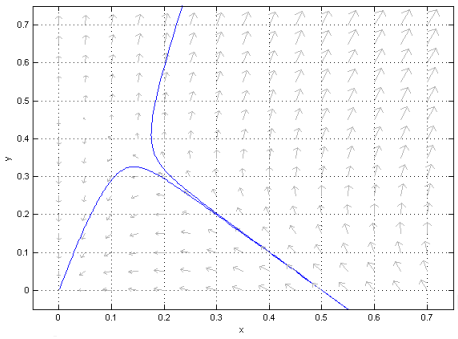

Figure 4: Phase plane for the evolution of the moment of f without well balancing, $s = 0.5$. It is apparent that the solution eventually will either converge to zero or become unbounded.

$$\frac{d}{dt}\left(f_1 + f_2\right) = \left(f_1 + f_2\right)^2 - \rho_0\left(f_1 + f_2\right).$$

Here the sum $f_1 + f_2$ is not constant in time, in fact we get two equilibrium solutions which are $f_1 + f_2 = 0$ and $f_1 + f_2 = \rho_0$. Moreover, the equilibrium $f_1 + f_2 = 0$ is always stable and attractive, while $f_1 + f_2 = \rho_0$ is unconditionally unstable. This means that mass conservation $f_1(t) + f_2(t) = \rho_0$ holds $\forall t$ if and only if there are no perturbations of the sum of the distribution functions, i.e. if $f_1(t) + f_2(t)$ is computed without roundoff. Therefore, in contrast with the first formulation (23) which gives a well-balanced scheme, in the second formulation (24) small perturbations of the sum $f_1 + f_2$ at the time t could affect mass conservation.

The situation is illustrated in Fig. 3, where the two equations (23) and (24) are integrated in time, starting with initial conditions giving $\rho = 0.3, \rho = 0.5$ and $\rho = 0.7$ respectively, for a 2 velocity classes problem. In the figure, the green curve corresponds to $f_2 = f(v_2)$, while the blue curve denotes $f_1 = f(v_1)$). Recall that $v_1 = 0$. It is easy to see that the equilibrium distribution should be $f = (0, \rho)$ in the two cases on the left, which have $s \leq \frac{1}{2}$, while it should settle on two constant states in the third case. It is apparent that the dashed line, which corresponds to the solution of (23) converges to the correct solution, while the functions obtained with (24) (solid line) are eventually driven by round off to the spurious equilibrium $(0, 0)$.

The phase plane for the two components of the solution (f_1, f_2) appearing in Fig. 4 show that any initial condition can be drawn to either $(0, 0)$ or become unbounded, for any slight perturbation.

5 Fundamental diagrams of 2-population models

In this section we will show the numerical results provided by the fundamental diagrams obtained with the 2-populations kinetic model (18). As we will see, these results not only account for the main qualitative features of the experimental data of Fig. 1, but they also provide tools to understand the behavior of traffic at a macroscopic scale.

In all cases, the space homogeneous time evolution of the distribution functions for the two populations are integrated numerically up to equilibrium, using the well balanced formulation (23). Once the equilibrium distributions have been obtained, the flow and the density are found

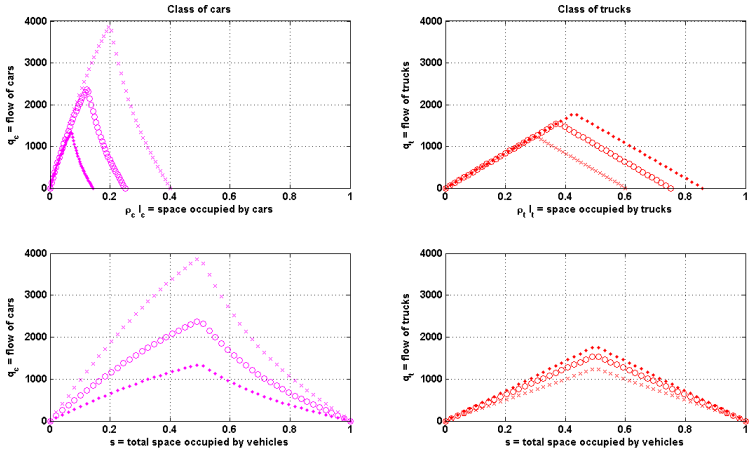

Figure 5: Flux-space diagram. At the top we have the flow versus the occupied space for each class of vehicles (cars on the left, trucks on the right). At the bottom we have the relation between the flux of each class of vehicles (cars on the left, trucks on the right) and the total occupied space s.

from the moments of the two distributions. Clearly, in the space homogeneous case, the density is constant, and therefore it is already known from the initial conditions.

We notice that there are two quantities which can be related to the flow in the fundamental diagram. It is possible to compute the flux as a function of s, defined in (17), to show the relation between the flux and the fraction of occupied space. However, it is also interesting to study the relation between the flow and the total density, defined as $\rho_C + \rho_T$, i.e. the flow as a function of the total number of vehicles at a given section of the road. In fact, we expect that experimental diagrams represent the flow-density relation.

More precisely,

- **flux-space diagrams**. These are diagrams of the total flux $F = \sum_{j=1}^{n} v_j f_j^e + \sum_{j=1}^{m} v_j g_j^e$, versus s, defined in (17).
- **flux-density diagrams**. These are obtained considering F as a function of the total density $\rho = \rho_T + \rho_C$, that is the total number of vehicles, per unit length, irrespective or the size of the different vehicles.

We start from flux-space diagrams. Except when explicitly indicated, all figures are obtained setting $\alpha = \eta = 1$ and $l_T = 3l_C$, where l_C, l_T are the lengths of vehicles of cars and trucks, respectively. Initially, we assume that cars have $n = 3$ speed classes, with maximum speed $v_3 = 100km/h$, and the corresponding velocity space is $V_C = \left\{v_j = \frac{j-1}{2}100\right\}_{j=1}^{3}$; while trucks have $m = 2$ speed classes, with maximum speed $v_2 = 50km/h$, thus $V_T = \{v_j = (j-1)50\}_{j=1}^{2}$. Thus in the first examples $V_C = \{0, 50, 100\}$, while $V_T = \{0, 50\}$.

In Figure 5 we show the flux-space diagrams obtained using deterministic initial conditions: for any given $s \in [0, 1]$, we give three values of $(\rho_C l_C, \rho_T l_T)$ such that $\rho_C l_C + \rho_T l_T = s$, representing typical cases. More precisely, in the set $\left\{(\rho_C l_C, \rho_T l_T) \in [0, 1]^2 : \rho_C l_C + \rho_T l_T \leq 1\right\}$ we choose the combinations in Table 1. We notice that the fundamental diagram of each class reproduces a diagram similar to the one provided by the 1-population model (4), with two and three velocity

Identifier	Combination type	Marker	Expression
1)	space is occupied mostly by cars	Crosses	$\rho_T l_T = \frac{1}{2}\rho_C l_C$
2)	space is occupied evenly by cars and trucks	Circles	$\rho_T l_T = \rho_C l_C$
3)	space is occupied mostly by trucks	Dots	$\rho_T l_T = 2\rho_C l_C$

Table 1: Deterministic combinations used in the figures, with the corresponding markers appearing in the plots

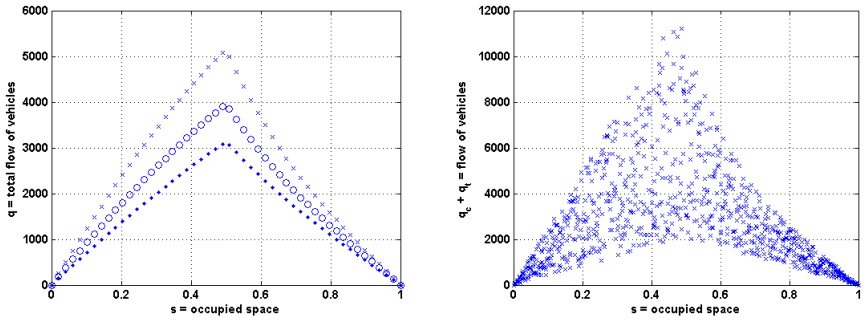

Figure 6: Flux-space diagrams for the total flow of vehicles. Left: for each fixed value of $s \in [0, 1]$, three deterministic initial conditions, corresponding to the combinations of Table 1. Right: three random initial conditions, for each fixed s.

classes; for instance, the diagram of trucks is a triangle, as we showed in Figure 2 for two classes of speed.

All plots in Fig. 5 show clearly that there is a critical fraction of occupied space, beyond which the flow starts to decrease. On the top section of the figure, the two subplots show that the critical space for each species changes depending on the mixture we consider. In fact, the space occupied by a class of vehicles is only one contribution to the fraction of occupied space which determines the transition matrices. In other words, even the dynamics of a single species depends on the dynamics of the complete mixture. Consequently, the flow depends on the composition of traffic.

In the bottom section of the figure, the flow of cars and trucks is shown as a function of the total fraction of occupied space s. One can immediately note that there is a single value for the critical space which corresponds to $s = \frac{1}{2}$ for all three combinations. This result seems to suggest that the transition from the free to the congested phase does not depend on how the road is occupied but on how much of it is occupied.

The left of Fig. 6 shows the total flow as a function of s, again, for the three combinations of Table 1, and for three random combinations, for each fixed s. Here the role of the critical value $s = \frac{1}{2}$ is even more apparent. This diagram does not reproduce the experimental data, because s does not provide information on the heterogeneity of traffic.

Now we will consider flux-density diagrams, which give the flux as a function of the number of vehicles per kilometer. In this case, the composition of traffic is taken into account, because the same fraction of occupied space $s \in [0, 1]$ can be obtained by different initial densities ρ_C, ρ_T.

For any given $s \in [0, 1]$, the plots in Figure 7 are obtained by taking initial conditions ρ_C, ρ_T such that $\rho_C l_C + \rho_T l_T = s$, where ρ_C and ρ_T are chosen according to the combinations of Table 1. The plot on the right gives the total flux as a function of the total number of vehicles. This deterministic choice allows us to look at the transition from free to congested phase. Here, each

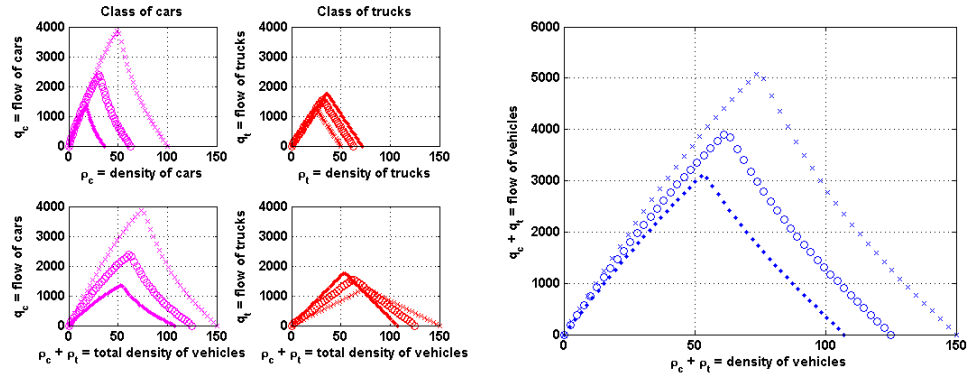

Figure 7: Left, flux-density diagrams for each class of vehicles versus vehicle class density (top row) or total density (bottom row), for the 3 deterministic combinations of Table 1. On the right, flux-density-diagram with total density on the x-axis and total flow of vehicles on the y-axis.

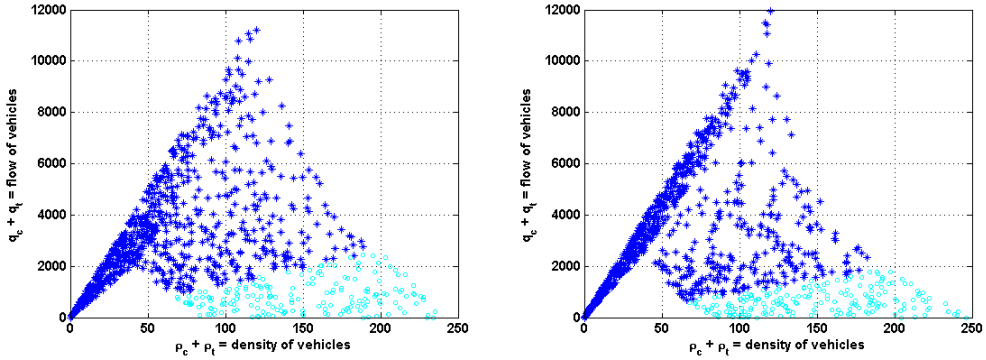

Figure 8: Flux-density diagram for the complete mixture, obtained with three random initial conditions ρ_C and ρ_T, for each value of s. On the left, $n = 3$ speed classes for cars and $m = 2$ speed classes for trucks; on the right, $n = 4$ and $m = 3$. We marked with blue *-symbols the flow values obtained with a fraction of occupied space less than 0.8, with cyan circles those provided by $s \in [0.8, 1]$.

combination has a different critical value of the density for the phase transition, which depends on the ratio of the different species within the mixture. But we know from Fig. 6 that each of these critical values of the density will correspond to the single value $s = \frac{1}{2}$. Note that the plot on the right begins to resemble the experimental fundamental diagrams of Fig. 1.

If we sample three random values of ρ_C, ρ_T for any given $s \in [0, 1]$, we obtain the flux-density diagram in Figure 8, and we note that now the main features of the phenomena discussed in Section 2 are captured: in particular, at low densities we have a linear increase of the flow with small dispersion; in contrast, in the congested phase, we have a large scattering of the flow values following the frequent interactions between fast and slow vehicles. In this figure, and in the following two, we indicated with cyan circles the values obtained for $s \in [0.8, 1]$, with blue crosses the data corresponding to $s \in [0, 0.8]$, which are the most likely to occur in practice, since even in traffic jams, traffic arrives seldom at a state of maximum density and complete stop, as shown also in Fig. 1, where a residual movement always appears.

Since the flow values depend on how the mixture is composed, we can state that the bulk

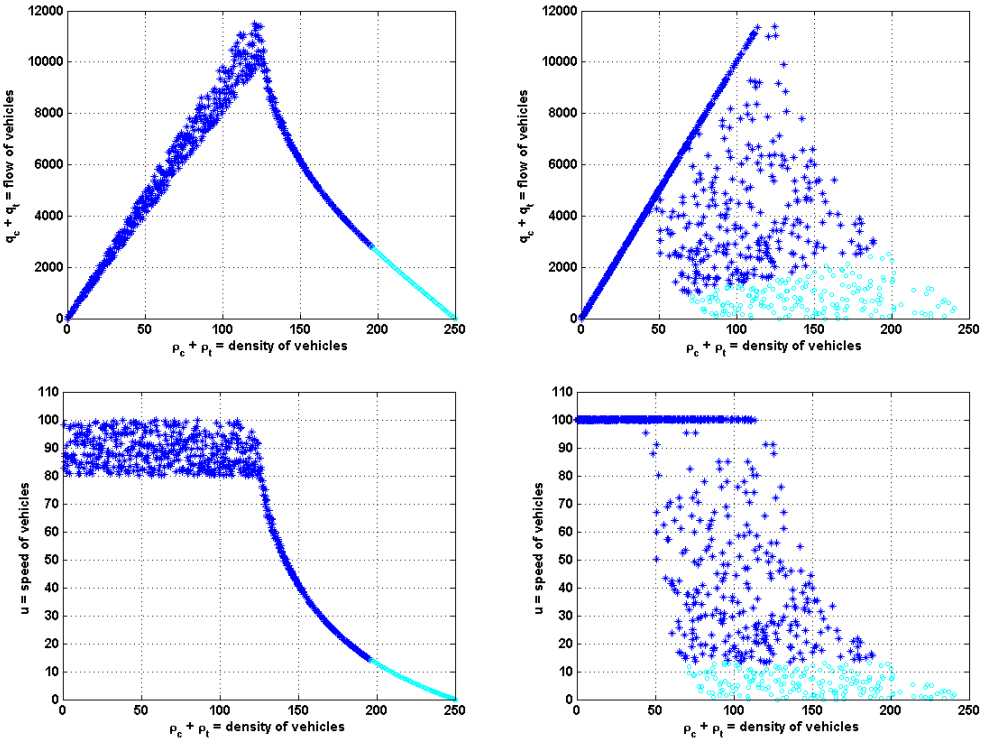

Figure 9: Flux-density diagram (top row) and average speed of the whole flow versus total density (bottom row) : on the left, the two classes of vehicles have the same lengths $l = 4$mt. and they differ in maximum velocity, in fact $V_C = [0, 50, 80, 100]$ and $V_T = [0, 50, 80]$; on the right, the two classes of vehicles differ in length, i.e. $l_C = 4$mt. $l_T = 12$mt., but $V_C = V_T$. Blue *: values with $s \in [0.8, 1]$, cyan circles $s \in [0.8, 1]$.

characteristics of traffic can be predicted deterministically, when the composition of traffic is known. In fact, if we give one pair (ρ_C, ρ_T) of initial values, we can compute *exactly* what the resulting flux will be. In this interpretation, the scattering of data in the congested phase is not due to the impredictability of the drivers' behavior, but it might be due to a lack of knowledge on the composition of traffic.

This affirmation can be articulated more precisely, by considering the 2-populations model (18) in which vehicles differ by only one characteristic. The plot on the left of Figure 9 shows the flux-density diagram when the two classes of vehicles have the same length, but they differ in their maximum speed: $V_C = [0, 50, 80, 100]$ and $V_T = [0, 50, 80]$. We can interpret this case as thinking that the vehicles are now identical, but we are considering two different types of driver, according to the maximum speed they are willing to settle on when the road is free. The plot on the right of Figure 9 is obtained by considering vehicle classes which have different lengths but the same microscopic speeds.

These results seem to suggest that, in order to describe the scattering of the data, the presence in the flow of a mixture of vehicles with different lengths accounts for the scattering of the data in the congested phase, while the presence of drivers with different driving habits accounts for the (small) scattering of data in the free flow phase. Note that this conclusion is indeed consistent

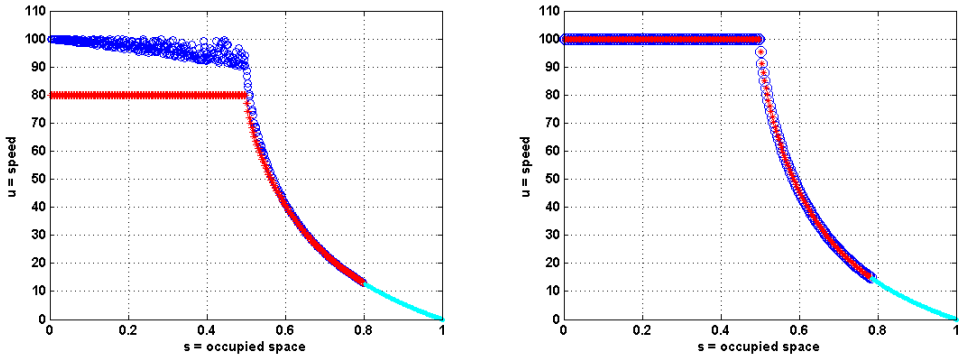

Figure 10: Average speed versus space occupied for the two populations: cars (blue) and trucks (red): on the left, the two classes of vehicles have the same lengths $l = 4$mt, with different velocity spaces $V_C = [0, 50, 80, 100]$ and $V_T = [0, 50, 80]$; on the right, the two classes of vehicles differ in length, i.e. $l_C = 4$mt. $l_T = 12$mt., but $V_C = V_T$. Blue *: values with $s \in [0.8, 1]$, cyan circles $s \in [0.8, 1]$.

with every day driving experiences: in the free flow phase, people drive at different speeds, while in the congested phase, everybody travels with the same speed, which decreases steadily as the congestion of the road increases.

The plots in Fig. 10 show the behavior of the average speed of each of the two populations, as a function of the occupied space. On the left, the vehicles have the same length, but $V_C = [0, 50, 80, 100]$ (blue data) and $V_T = [0, 50, 80]$ (red markers). The slow population is not affected by the presence of the fast cars, but the fast cars do interact with the slow population, until the road becomes congested, and both types of drivers slow down, keeping the same average speed. Again, this represents a familiar phenomenon. On the right, we find the average speed of each population, in the case in which the velocity spaces are the same, but the lengths of the vehicles are different. In this case, the average speed is the same for both types of drivers, and depends only on the fraction of occupied space.

Finally, we emphasize that the kinetic approach seems to be essential in order to describe the sharp transition phase we observe. We draw flux-density diagrams for the complete mixture in the 2-population macroscopic model of [5], summarized by eq. (11), obtaining the plot in Fig. 11. Here, we can easily note that there is no trace of the sharp phase transition which appeared in the kinetic model, and the scattering of the data is very high also at low denisties.

6 Conclusions and perspectives

We have introduced a kinetic model for vehicular traffic flow with a new and more detailed structure which accounts for the heterogeneous composition of the flow of vehicles. Our approach differs from standard kinetic models in that we consider two distribution functions describing two classes of objects with different physical features, e.g. the vehicle typical length and its maximum possible speed.

As in [8], the model is built by assuming a discrete velocity space and the possible interactions between vehicles are weighted by suitable transition probabilities. We show that our model satisfies an indifferentiability principle, which makes the 2-population case consistent with the original single population model, when the particles composing the mixture share the same

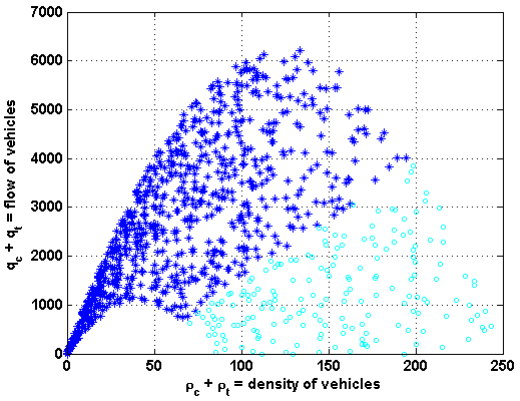

Figure 11: Flux-density diagram for the macroscopic model (11) for the complete mixture, obtained giving three random initial conditions ρ_1 and ρ_2, for each given value of s. Blue *: values with $s \in [0.8, 1]$, cyan circles $s \in [0.8, 1]$.

physical properties. This property, enforced in [1], is not trivial, and several kinetic models for gas mixtures possess it only at equilibrium, [13, 15].

We compute the equilibria of the system, and we use the equilibrium distribution to derive the fundamental diagrams of the proposed model. Even with a small number of microscopic speeds, the resulting fundamental diagrams are endowed with a structure resembling experimental data. These are characterised by a marked phase transition, as described also in Section 2 when discussing experimental data: at low densities (free flow) the flow can be linearly approximated with a small standard deviation, while beyond a critical state, the flow decreases, and the data become widely scattered (congested phase).

Several authors have dealt with this problem, see [9] or [14] accounting for this phenomenon for instance with the uncertainty in the driver's behavior modeled with the standard deviation of the distribution function. However, in this case the single population model provides a zero standard deviation in the free phase of traffic. In our case, we recover a sharp phase transition, which seems to come naturally from a kinetic modelling, but we also obtained the scattered behavior as a consequence of the fact that a given road occupancy can be obtained with different compositions of the mixture. In other words, if the flux is given as a function of the number of vehicles crossing a section in a unit of time, the scattering may be due to the presence of different type of vehicles. On the other hand, in the congested phase, the average speed of the drivers seem to depend only on the degree of congestion of the road.

From the point of view of applications, our results can be used to direct the strategies of data collection in experimental research on traffic flow. In fact, other types of fundamental diagrams can be studied, relating the number of vehicles not only to the flow, as is currently done. For example, with a multi-population model, it is possible to study the volume of goods transported by trucks in a current of cars, or the number of passengers carried by a flow composed of cars and buses.

Finally, we also wish to note that the model is very simple: the complexity of the real flow is clustered in the characteristics of only two distinct populations, with a very small number of microscopic velocities. Thus, from a computational point of view, this construction is not significantly more demanding than a macroscopic model.

We can prove that the model introduced in this work is well posed, in the sense that the dis-

tribution functions remain positive and bounded by their initial mass. Further, it is also possible to prove that the equilibria are uniquely defined by the initial mass of the two distributions, and, in some simplified cases, they can be explicitly computed. These results will be gathered in a forthcoming paper [28]. Further study will be dedicated to the extension of these models to road networks and multilane highways.

References

[1] P. Andries, K. Aoki, and B. Perthame. A consistent BGK-type model for gas mixtures. Technical report, Institut National De Recherche En Informatique Et En Automatique, 2001. Rapport de recherche n°4230.

[2] A. Aw, A. Klar, T. Materne, and M. Rascle. Derivation of continuum traffic flow models from microscopic follow-the-leader models. *SIAM J. Appl. Math.*, 63(1):259–278, 2002.

[3] A. Aw and M. Rascle. Resurrection of "second order" models of traffic flow. *SIAM J. Appl. Math.*, 60(3):916–938 (electronic), 2000.

[4] N. Bellomo and C. Dogbé. On the modelling of traffic and crowds. A survey of models, speculations, and perspectives. *SIAM Rev.*, 53(3):409–463, 2011.

[5] S. Benzoni-Gavage and R.M. Colombo. An n-populations model for traffic flow. *European Journal of Applied Mathematics*, 14(05):587–612, 2003.

[6] S. Brull, V. Pavan, and J. Schneider. Derivation of a BGK model for mixtures. *European Journal of Mechanics B/Fluids*, 33:74–86, 2012.

[7] M. Delitala and A. Tosin. Mathematical modeling of vehicular traffic: a discrete kinetic theory approach. *Math. Models Methods Appl. Sci.*, 17(6):901–932, 2007.

[8] L. Fermo and A. Tosin. A fully-discrete-state kinetic theory approach to modeling vehicular traffic. *SIAM J. Appl. Math.*, 73(4):1533–1556, 2013.

[9] L. Fermo and A. Tosin. Fundamental diagrams for kinetic equations of traffic flow. *Discrete Contin. Dyn. Syst. Ser. S*, 7(3):449–462, 2014.

[10] M. Garavello and B. Piccoli. *Traffic flow on networks*, volume 1 of *AIMS Series on Applied Mathematics*. American Institute of Mathematical Sciences (AIMS), Springfield, 2006.

[11] M. Garavello and B. Piccoli. *Traffic Flow on Networks – Conservation Laws Models*. AIMS Series on Applied Mathematics. American Institute of Mathematical Sciences (AIMS), Springfield, MO, 2006.

[12] D.C. Gazis, R. Herman, and R.W. Rothery. Nonlinear follow-the-leader models of traffic flow. *Operations Res.*, 4:545–567, 1961.

[13] M. Groppi and G. Spiga. A BGK-type approach for chemically reacting gas mixtures. *Physics of Fluids*, 16(12):4273–4284, 2004.

[14] M. Günther, A. Klar, T. Materne, and R. Wegener. Multivalued fundamental diagrams and stop and go waves for continuum traffic flow equations. *SIAM J. Appl. Math.*, 64(2):468–483 (electronic), 2003/04.

[15] B.B. Hamel. Kinetic model for binary gas mixtures. *Physics of Fluids*, 8:418–425, 1965.

[16] M. Herty, C. Kirchner, and A. Klar. Instantaneous control for traffic flow. *Math. Methods Appl. Sci.*, 30(2):153–169, 2007.

[17] B.S. Kerner. *The Physics of Traffic*. Springer, Berlin, 2004.

[18] A. Klar and R. Wegener. A hierarchy of models for multilane vehicular traffic. I. Modeling. *SIAM J. Appl. Math.*, 59(3):983–1001 (electronic), 1999.

[19] A. Klar and R. Wegener. A hierarchy of models for multilane vehicular traffic. II. Numerical investigations. *SIAM J. Appl. Math.*, 59(3):1002–1011 (electronic), 1999.

[20] A. Klar and R. Wegener. Traffic flow: models and numerics. In *Modeling and computational methods for kinetic equations*, Model. Simul. Sci. Eng. Technol., pages 219–258. Birkhäuser Boston, Boston, MA, 2004.

[21] R.J. Leveque. Balancing source terms and flux gradients in high-resolution godunov methods: the quasi-steady wave-propagation algorithm. *J. of Comp. Phys.*, 146:346–365, 1998.

[22] M.J. Lighthill and G.B. Whitham. On kinematic waves. II. A theory of traffic flow on long crowded roads. *Proc. Roy. Soc. London. Ser. A.*, 229:317–345, 1955.

[23] S. Noelle, Y. Xing, and C.W. Shu. Well-balanced schemes for moving water. 1 high order well-balanced finite volume weno schemes for shallow water equation with moving water.

[24] S. L. Paveri-Fontana. On Boltzmann-like treatments for traffic flow: a critical review of the basic model and an alternative proposal for dilute traffic analysis. *Transportation Res.*, 9(4):225–235, 1975.

[25] B. Piccoli and A. Tosin. Vehicular traffic: a review of continuum mathematical models. In *Encyclopedia of Complexity and Systems Science*, volume 22, pages 9727–9749. Springer, New York, 2009.

[26] I. Prigogine. A Boltzmann-like approach to the statistical theory of traffic flow. In *Theory of traffic flow*, pages 158–164. Elsevier, Amsterdam, 1961.

[27] I. Prigogine and R. Herman. *Kinetic theory of vehicular traffic*. American Elsevier Publishing, New York, 1971.

[28] G. Puppo, M. Semplice, A. Tosin, and G. Visconti. An heterogeneous kinetic model for traffic flow. Technical report. in preparation.

[29] P.I. Richards. Shock waves on the highway. *Operations Res.*, 4:42–51, 1956.

[30] B. Seibold, M.R. Flynn, A.R. Kasimov, and R.R. Rosales. Constructing set-valued fundamental diagrams from jamiton solutions in second order traffic models. *AIMS Networks and Heterogeneous Media*, 8(3):745–772, 2013.

[31] Transportation Research Board. *75 Years of the Fundamental Diagram for Traffic Flow Theory*, June 2011. CIRCULAR E-C149.